## **Dual-band Optical Isolation in Thin-film Lithium Niobate Based on Dynamic Modulation**

## Manav Shah,\* Ian Briggs, Pao-Kang Chen, Songyan Hou, and Linran Fan

James C. Wyant College of Optical Sciences, The University of Arizona, 1630 E. University Blvd., Tucson, AZ 85721, USA

\*manavshah@optics.arizona.edu

Current integrated optical isolators have limited bandwidths due to stringent phase-matching, resonant structures, or absorption. We demonstrate broadband optical isolation in thin-film lithium niobate that simultaneously achieves  $\sim 100$  nm isolation bandwidth at visible and telecom wavelengths. © 2023 The Author(s)

Optical isolators are described by a non-reciprocal, asymmetric scattering matrix that breaks Lorentz reciprocity [1]. Bulk-optical isolators convert non-reciprocal magneto-optical phase shift to unidirectional transmission or mode conversion. Analogous integrated isolators have been demonstrated by integrating yttrium iron garnets with various photonic platforms [2]. Alternative integrated isolators have also been proposed based on nonlinear processes and dynamic traveling-wave modulation [3]. But nearly all of the above approaches require stringent phase-matching, interferometric structures, or material absorption that severely limit the isolation bandwidth of the devices. In contrast, dynamic standing-wave modulation in a tandem configuration has been shown to achieve a high isolation ratio and large bandwidth, limited only by the optical bandwidth of modulation [4, 5]. Here, we demonstrate a broadband, integrated optical isolator in thin-film lithium niobate (LN) based on this design that can achieve a high isolation ratio, minimal optical distortion, flexible design, and real-time tunability.

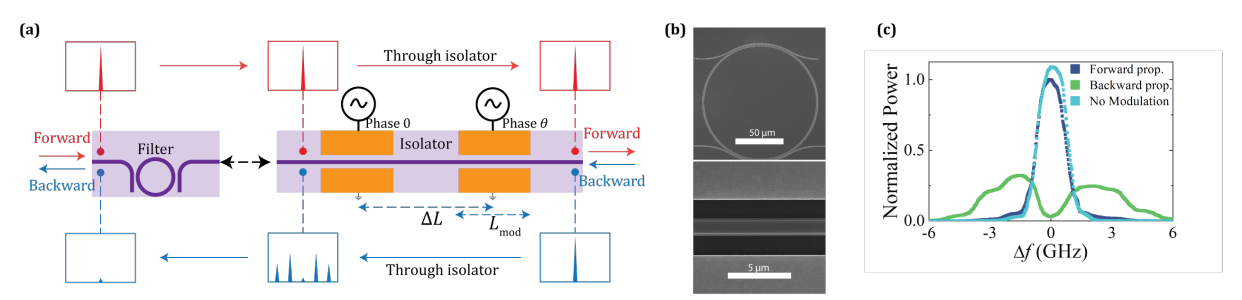


Fig. 1. (a) Schematic of the optical isolator. (b) Scanning electron microscopy of the micro-ring add/drop filter and electro-optic modulator fabricated on thin film LN. (c) Measured data from optical spectrum analyzer (OSA).

The schematic in Fig. 1a shows the design of the isolator. Two standing-wave modulators separated by an optical delay line  $(\Delta L)$  are driven with a mutual microwave phase difference  $\theta$  and microwave frequency  $F_{\rm m}$ . The length of the delay line is fixed to  $\Delta L = c/4F_{\rm m}n_{\rm g}$ , where  $n_{\rm g}$  is the group refractive index for the fundamental transverse electric optical mode of the thin-film LN waveguide. If the modulators are driven with amplitude A, the forward  $(T_{\rm f})$  and backward  $(T_{\rm h})$  transmissions for the optical mode are given by

$$T_{f}(t) = e^{i2A\cos\left[2\pi F_{m}t + \left(\frac{\theta - 2\pi F_{m}\Delta T}{2}\right)\right]\cos\left(\frac{\theta + 2\pi F_{m}\Delta T}{2}\right)}, \qquad (1)$$

$$T_{b}(t) = e^{i2A\cos\left[2\pi F_{m}t + \left(\frac{\theta - 2\pi F_{m}\Delta T}{2}\right)\right]\cos\left(\frac{\theta - 2\pi F_{m}\Delta T}{2}\right)}. \qquad (2)$$

$$T_{\rm b}(t) = e^{i2A\cos\left[2\pi F_{\rm m}t + \left(\frac{\theta - 2\pi F_{\rm m}\Delta T}{2}\right)\right]\cos\left(\frac{\theta - 2\pi F_{\rm m}\Delta T}{2}\right)}.$$
 (2)

where the optical delay  $\Delta T = \Delta L/c$ . If  $\theta$  is chosen such that  $\theta + 2\pi F_{\rm m}\Delta T = 0$ , the forward transmission  $T_{\rm f}(t) = 1$ , while the backward transmission is phase-modulated and can be expanded into constituent frequency components

$$T_{\rm b}(t) = \sum_{k} i^{k} J_{k} \left[ 2A \cos\left(\frac{\theta - 2\pi F_{\rm m} \Delta T}{2}\right) \right] e^{ik\left(2\pi F_{\rm m}t + \frac{\theta - 2\pi F_{\rm m} \Delta T}{2}\right)}, \tag{3}$$

where the amplitude of the  $k^{\text{th}}$  frequency band is given by the  $k^{\text{th}}$  order bessel function of the first kind  $(J_k)$ . The backward transmission at the optical center frequency (k=0 band) may be suppressed by satisfying the condition

$$J_0 \left[ 2A \cos \left( \frac{\theta - 2\pi F_{\rm m} \Delta T}{2} \right) \right] = 0. \tag{4}$$

Typically, Eq. 4 is satisfied by setting  $A = 0.385\pi$  and  $\theta = 2\pi F_{\rm m}\Delta T = \pi/2$ . The device thus functions as an optical isolator at the optical center frequency. Due to the absence of phase matching or resonance constraints in Eq. 4, this isolator can operate across the entire wavelength range of modulation (visible to near-infrared wavelengths).

We fabricated this device in thin-film LN using electron-beam lithography and Ar plasma etching for the optical waveguides, and Au evaporation followed by liftoff in acetone for the microwave electrodes (Fig. 1b). The device transmission is measured using an OSA (Fig.1c). We measured an isolation ratio of 15 dB at wavelength  $\lambda = 1550$  nm and an insertion loss below 0.5 dB. To test the isolation at visible wavelengths, we introduced an integrated micro-ring filter with a passband of 1.25 GHz and 1 GHz at  $\lambda = 1550$  and 775 nm, respectively. The passband was thermally tuned to scan the transmission frequency bands around the optical center frequency. Figures 2a,b show the measured backward transmission at  $\lambda = 1550$  and 775 nm without changing the microwave drive. The resultant isolation ratios measured through the filter are 7 dB and 5 dB for  $\lambda = 1550$  and 775 nm, respectively. The lower isolation ratio for  $\lambda = 1550$  nm compared to the OSA measurement is due to the larger bandwidth of the micro-ring filter. Additionally, the mismatch between the  $n_g$  at  $\lambda = 1550$  and 775 nm means that Eq. 4 is not perfectly satisfied for  $\lambda = 775$  nm, further lowering the isolation ratio at  $\lambda = 775$  nm. Nonetheless, our calculations show that this isolator can show simultaneous dual-band isolation around  $\lambda = 1550$  and 775 nm, with 10 dB isolation bandwidths of  $\sim 100$  nm around the center wavelengths (Fig. 2c). This dual-band isolation is ideal for nonlinear integrated photonics applications like second harmonic generation and parametric down-conversion. The flexibility in the choice of  $F_{\rm m}$  and  $\theta$  provides robust tolerance for any practical application of this isolator (Fig. 2d). Moreover, the isolation direction can be switched by simply reversing the parity of  $\theta$ .

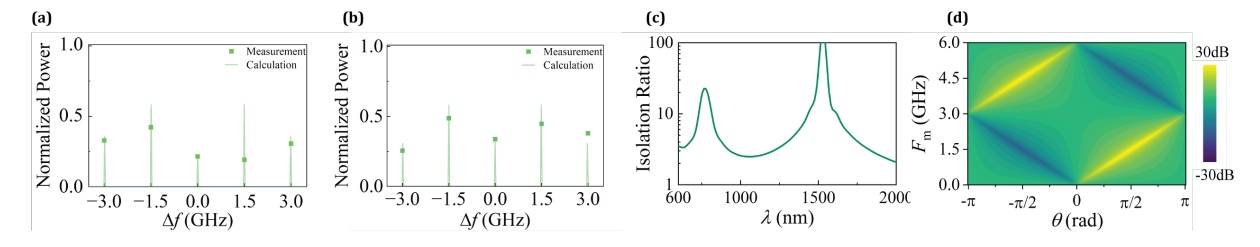


Fig. 2. (a) Normalized telecom and (b) normalized visible transmission for backward propagation measured using the tunable micro-ring filter. (c) Calculated isolation ratio for visible and telecom wavelengths, optimized for  $\lambda=1550$  nm. (d) Isolation ratio at  $\lambda=1550$  nm for varied  $F_{\rm m}$  and  $\theta$ .

In conclusion, we demonstrated broadband optical isolation in thin-film LN using tandem standing-wave modulation, which can simultaneously operate at visible and telecom wavelengths. The high isolation ratio, low insertion loss, flexible design and operation, and real-time tunability make this isolator an excellent choice for photonic integrated circuits in thin-film LN.

## References

- 1. D. Jalas, A. Petrov, M. Eich, W. Freude, S. Fan, Z. Yu, R. Baets, M. Popović, A. Melloni, J. D. Joannopoulos *et al.*, "What is—and what is not—an optical isolator," Nat. Photonics **7**, 579–582 (2013).
- 2. Y. Zhang, Q. Du, C. Wang, T. Fakhrul, S. Liu, L. Deng, D. Huang, P. Pintus, J. Bowers, C. A. Ross, J. Hu, and L. Bi, "Monolithic integration of broadband optical isolators for polarization-diverse silicon photonics," Optica 6, 473 (2019).
- 3. I. A. D. Williamson, M. Minkov, A. Dutt, J. Wang, A. Y. Song, and S. Fan, "Integrated Nonreciprocal Photonic Devices With Dynamic Modulation," Proc. IEEE 108, 1759–1784 (2020).
- 4. C. R. Doerr, N. Dupuis, and L. Zhang, "Optical isolator using two tandem phase modulators," Opt. Lett. **36**, 4293
- C. R. Doerr, L. Chen, and D. Vermeulen, "Silicon photonics broadband modulation-based isolator," Opt. Express 22, 4493 (2014).